Title: Cerberus-Nodal-Lefty-Pitx signalling cascade controls Left-Right asymmetry in amphioxus

Short title: Left-Right asymmetry in amphioxus

Guang Li[1, §], Xian Liu[1, §], Chaofan Xing[1], Huayang Zhang[1], Sebastian M. Shimeld[2*], Yiquan Wang[1*]

[1] State Key Laboratory of Cellular Stress Biology, School of Life Sciences, Xiamen University, Xiangan District, Xiamen, Fujian 361102, China
[2] Department of Zoology, University of Oxford, The Tinbergen Building, South Parks Road, Oxford OX1 3PS, UK
§ These authors contributed equally to this work.
* Corresponding authors: wangyq@xmu.edu.cn, sebastian.shimeld@zoo.ox.ac.uk

Supplementary Information Appendix

Materials and Methods

Larval cultivation and detection of *Cer* mutations in founder and F1 amphioxus

Embryos injected with TALEN mRNAs targeting *Cer* were reared at 24˚C in 5 litre plastic barrels filled with about 4 litres of filtered sea water and supplied with continuous air bubbling. After mouth opening, these larvae (we call them founders) were fed with unicellular algae *Dicrateria zhanjiangensis* (5-20 ml per time) twice a day. By 20 days after fertilization (around 8-gill slit stage), the animals were supplied with fine sand (2 cm thick) and fed with unicellular algae mixtures (*Platymonas sp*. and *Dicrateria zhanjiangensis*) twice a day. After metamorphosis (about 40 days after fertilization), the juveniles were reared as previous description (1, 2) till gonads became obvious. When the gonads developed to medium/large sizes, they were transferred to 20 ˚C plastic barrels for at least one week rearing before spawning induction (1). Gametes of each founder were collected individually and crossed with a wild-type animal respectively. After mid-neurula stage, 30-50 embryos of each cross were collected and analysed by PCR using Animal Tissue Direct PCR Kit (Foregene Co., China). Mutation efficiency and mutant sites of individuals were determined by restricted digestion and sequencing as previously described (1). The progeny (F1) carrying frame-shift mutations were maintained. When F1 grew up to around 3 centimetres in length, a tiny of individual tail tips were cut off for PCR amplification using above kit. After mutation diagnosis with restriction endonucleases, the mutation type of each individual was further determined by sequencing. Animals carrying identical frame-shift mutation were reared in a same tank, and inbreeding was carried out to generate F2 generation when F1 grew up to ripe adults, The F2 embryos were fixed at required developmental stages with 4% PFA-MOPS-EGTA (wt/vol) for *in situ* hybridization analysis or morphological examination.

Plasmid construct preparation

To clone the full-length coding sequences of *Cer*, *Nodal*, *Lefty* and *Pitx* genes into relevant expression vectors, a set of primers embedded with different restriction enzyme sites were synthesized according to the sequence data retrieved from the NCBI database. The coding sequences of each gene were separately amplified from a gastrula cDNA library and then ligated into a pGEM-T-Easy vector (Promega Co.). After verification by sequencing, each of the coding sequences was cut off from the pGEM-T-Easy construct and ligated into an expression vector pXT7. Sequences were also re-amplified from the pGEM-T-Easy constructs, and cloned into a modified P1 construct restricted by *BamH*I and *Spe*I to generate *Hsp70::Cer*, *Hsp70::Nodal*, *Hsp70::Lefty* and *Hsp70::Pitx* constructs. The P1 construct was initially made from the vector pAcGFP1-1 (Clontech Co.) by integrating a 790 bp regulatory region of *B. belcheri Hsp70* gene upstream the GFP coding sequence in our previous study (3), and was modified by adding a *Spe*I site after GFP stop codon. To make a *Pitx* dominant negative construct, we first cloned the *Drosophila* Engrailed repressor domain (EnR) into the pXT7 vector, and then inserted sequence encoding Pitx DNA-binding domain ahead of the EnR encoding region. TALENs targeting *Cer* and *Lefty* genes were designed and assembled as previously described (3).

SB505124 and Nodal protein treatment

SB505124 (Sigma Co.) was dissolved at 20 mM in dimethyl sulfoxide (DMSO) and recombinant mouse Nodal protein (R&D Co.) was dissolved at 250 ng/μL in sterile 1 mM HCL containing 0.2% bovine serum albumin. Embryos were treated with 50 μM SB505124 or 8 μg/ml Nodal protein (final concentration) in four-well dishes (coated with 1.5% agarose (wt/vol)) from early gastrula, and then washed with filtered seawater three times. Before the treatment, fertilization envelope was removed by pipetteing embryos very gently with a yellow micropipette tip to facilitate the reagent accessing the embryo. Embryos were also treated with equal amounts of DMSO or 1 mM HCL and used as a negative control. The treated embryos were collected and fixed at either 3- or 8-somite stages for *in situ* hybridization analysis, or cultured continuously for morphological phenotype observation.

***In situ* hybridization**

Embryos at desired developmental stages were fixed in 4% PFA-MOPS-EGTA (wt/vol) and then stored in 80% ethanol (vol/vol) in PBS at -20°C until needed. The pGEM-T-derived plasmids containing amphioxus *Cer*, *Nodal*, *Lefty* or *Pitx* coding regions were linearized by restriction enzyme digestion and applied to synthesize a digoxigenin (DIG)-labeled (Roche Co.) antisense riboprobe with Sp6 or T7 RNA polymerase (Promega, USA). Whole-mount *in situ* hybridization (WISH) was performed essentially as previously described (5). After staining, the embryos were washed with PBS, mounted in 80% glycerol (vol/vol) and photographed using an inverted microscope (Olympus Co.).

References

1. Li G, Shu Z, & Wang Y (2013) Year-round reproduction and induced spawning of Chinese amphioxus, Branchiostoma belcheri, in laboratory. *PLoS One* 8(9):e75461.
2. Li G, Yang X, Shu Z, Chen X, & Wang YQ (2012) Consecutive spawnings of Chinese amphioxus, Branchiostoma belcheri, in captivity. *PLoS One* 7(12):e50838.
3. Li D, *et al.* (2012) Isolation and functional analysis of the promoter of the amphioxus Hsp70a gene. *Gene* 510(1):39-46.
4. Li G, *et al.* (2014) Mutagenesis at specific genomic loci of amphioxus Branchiostoma belcheri using TALEN method. *J Genet Genomics* 41(4):215-219.
5. Yu JK & Holland LZ (2009) Amphioxus whole-mount in situ hybridization. *Cold Spring Harb Protoc* 2009(9):pdb prot5286.

Supplementary Tables

Table S1. Primers used for making pGEM-T Easy and pXT7 constructs

Genes	Primer sequences (5'→3')	Enzyme site added
Cer	Forward: GGTACCATGAAGACGAGCGTGAGGAGC	*Kpn*I
	Reverse: ACTAGTTCAGAAGTACTTATCCCCACATG	*Spe*I
Nodal	Forward: GGTACCGCAGGCCGAGACCAACACCGC	*Kpn*I
	Reverse: ACTAGTCTACTGACAGCCGCATTCATCC	*Spe*I
Lefty	Forward: CTCGAGTACGATGAAACCTGTTCTAGTT	*Xho*I
	Reverse: ACTAGTTTACTGTGTGCACGCACACTG	*Spe*I
Pitx	Forward: GGTACCACATATCTAAGGAGGACATCGTG	*Kpn*I
	Reverse: ACTAGTTCTTTAGCAAACAAATCCCATACGC	*Spe*I

Table S2. Primers used for making Hsp70 constructs

Genes	Primer sequences (5'→3')	Enzyme site added
Lefty	Forward: GGATCCTACGATGAAACCTGTTCTAGTT	*Bam*HI
	Reverse: GCGGCCGCACTAGTTTACTGTGTGCACGCACACTG	*Not*I-*Spe*I
Cer	Forward: GGTACCATGAAGACGAGCGTGAGGAGC	*Kpn*I
	Reverse: ACTAGTTCAGAAGTACTTATCCCCACATG	*Spe*I
Nodal	Forward: GGATCCGCAGGCCGAGACCAACACCGC	*Bam*HI
	Reverse: GCGGCCGCCTACTGACAGCCGCATTCATCC	*Not*I
Pitx	Forward: GGTACCACATATCTAAGGAGGACATCGTG	*Kpn*I
	Reverse: ACTAGTTCTTTAGCAAACAAATCCCATACGC	*Spe*I

Table S3. Primers used for making *Pitx-EN* construct

Genes	Primer sequences (5'→3')	Enzyme site added
Pitx	Forward: GGTACCACATATCTAAGGAGGACATCGTG	*Kpn*I
	Reverse: GAATTCTCCCAGCTGATTTCGCTCGCG	*EcoR*I

Table S4. Primers used for amplifying gene fragments including TALEN target sites

Genes	Primer sequences (5'→3')	Amplicon sizes (bp)
Cer	Forward: ATGAAGACGAGCGTGAGGAGC	427
	Reverse: CATCATCACCTGGAAGACGG	
Lefty	Forward: GAAACCTTCGCAGCAACATCG	376
	Reverse: CGACACGGGTAATTTGGAGC	

Table S5. *Cer* and *Lefty* TALEN binding sequences

Target gene	Target site sequence	Restriction enzyme used
Cer	TTTCAGACTCTCGGGTTGATT*CGGCCG*CCAGTCGGGAGGGGTCGGGACGGA	*Eag*I
Lefty	TTCTCGTGTGTTCTGGCCAGCG*CCTTGG*CGTTCTCGGCGGACCACGTCA	*Sty*I

Supplementary Figures

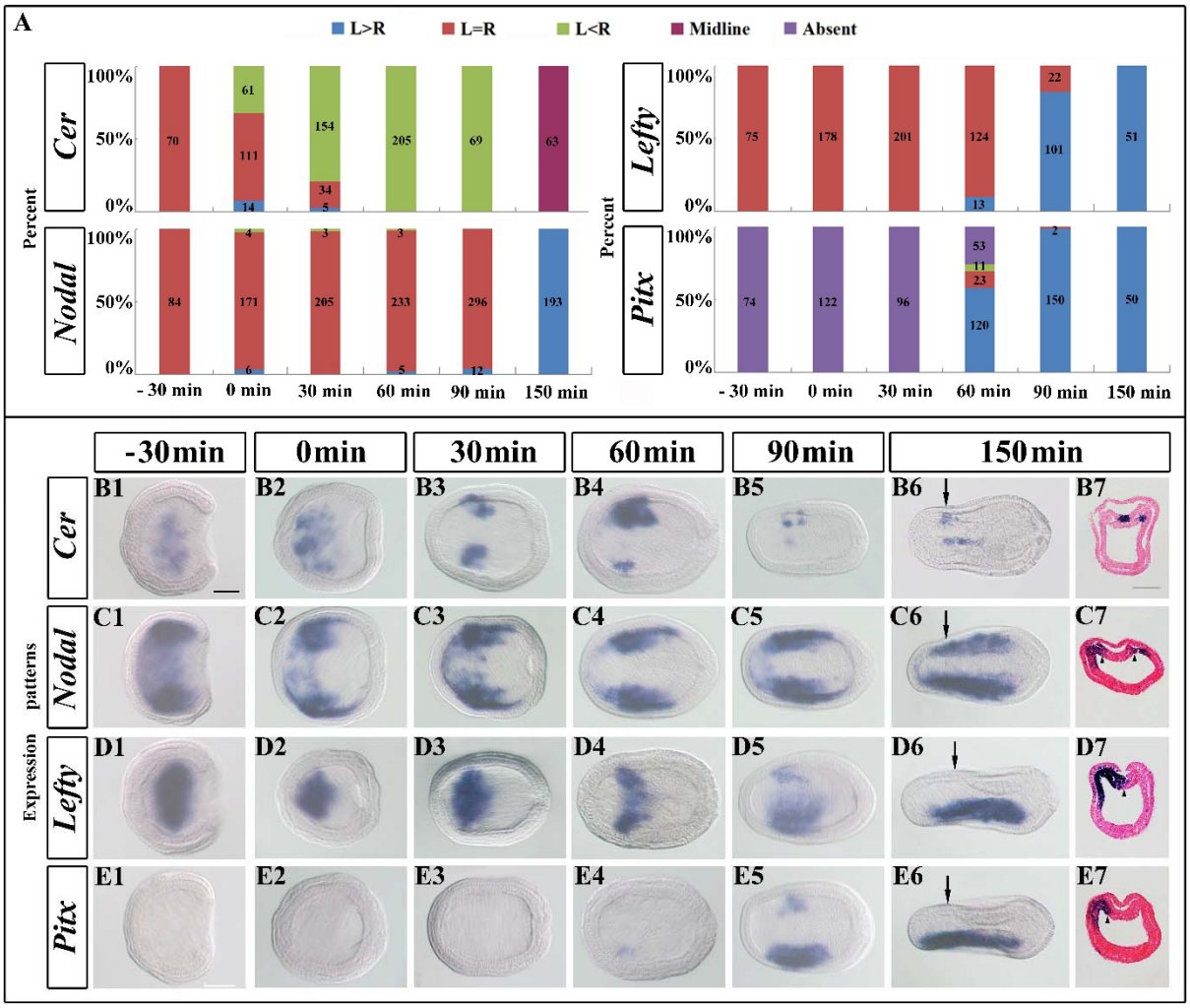

Fig. S1. Sequential onset of asymmetric expression of *Cer*, *Nodal*, *Lefty* and *Pitx* in amphioxus embryos. (A) Percentages of embryos showing each type of expression patterns (L>R, L = R, L < R and absent) for *Cer*, *Nodal*, *Lefty* and *Pitx* at 6 developing stages. Time at the late gastrula stage is defined as the 0 minute, and one stage before and 4 stages after that were adopted in the analysis. Following *in situ* hybridization, embryos were classified into right bias (R > L), equal distribution (R = L), left bias (R < L), or none (absent) of signals across the LR axis. Bars represent percentages; numbers of embryos analyzed are indicated on each bar. (B1-B6) Representative examples of *Cer* expression patterns at six developing stages. Arrow in (B6) marks the section plane in (B7). (B7) Transverse section of an embryo, showing *Cer* expression in the floor plate and several cells of the right first pre-somite. (C1-C6) Representative examples of *Nodal* expression patterns at six developing stages, note symmetric expression through early stages, with higher left-sided expression only visible in the oldest embryos. Arrow in (C6) marks the section plane in (C7). (C7) Transverse section of en embryo, showing *Nodal* expression in the left and right pre-somites. (D1-D6) Representative examples of *Lefty* expression patterns at six developing stages. Arrow in (D6) marks the section plane in (D7). (D7) Transverse section of an embryo, showing *Lefty* expression in the left first pre-somite and the regions adjacent to it, including the left side of dorsal-lateral endoderm, axial mesoderm and ectoderm. (E1-E6) Representative examples of *Pitx* expression patterns at six dveloping stages. Arrow in (E6) marks the section plane in (E7). (E7) Transverse section of an embryo, showing *Pitx* expression in the left pre-somites. Images in panels B, C, D and E are taken from the dorsal view with anterior to left. Scale bar (50 μm) in B1 applies to all panels.

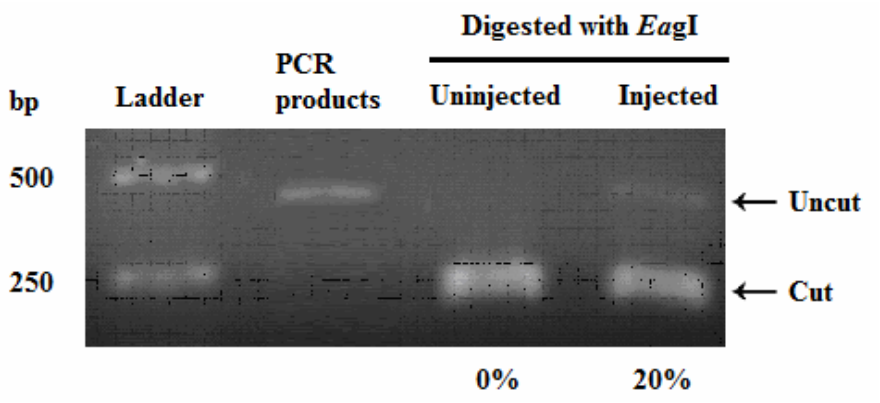

Fig. S2. Mutation rates of *Cer* TALEN in F0 embryos. Aout 30 embryos at mid-neurula stage were randomly collected for DNA extraction and PCR amplification. PCR products were digested with *Eag*I (which cuts within the TALEN engineered segment of DNA: see *SI Appendix*, Fig. S3). The uncut:cut ratio was estimated roughly as an indication of the mutation efficiency and labeled below the gel image. As expected, PCR products from the uninjected embryos were completely cut by *Eag*I, but approximately 20% of PCR products from the TALEN mRNA injected embryos were uncut.

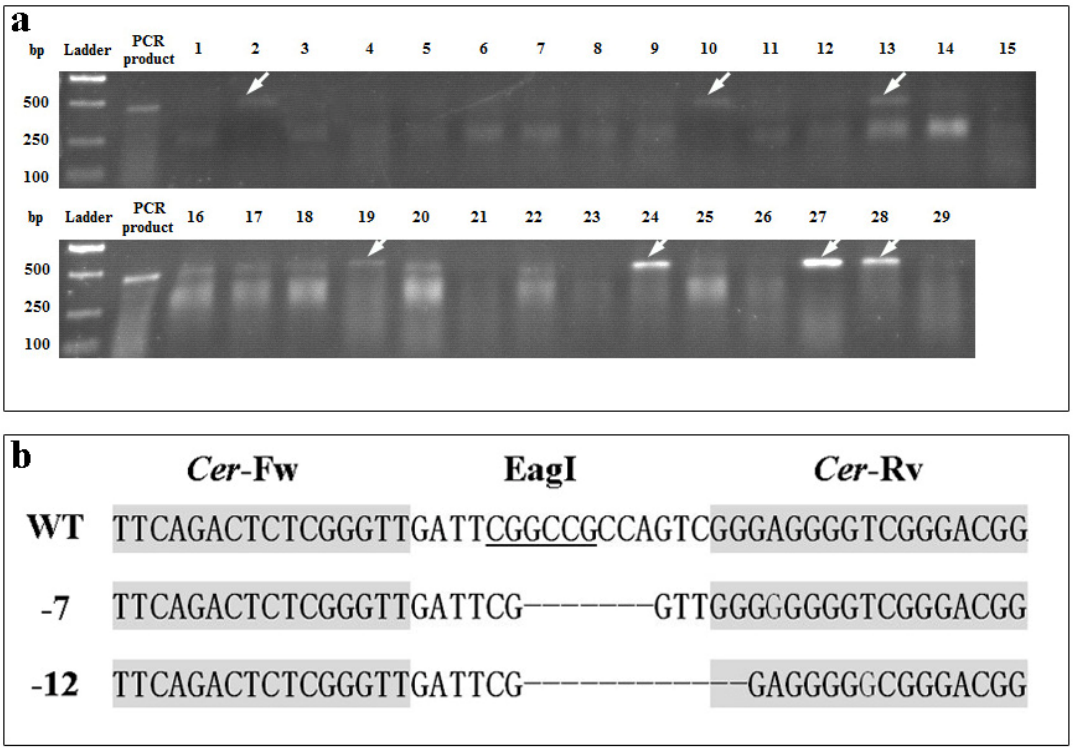

Fig. S3. *Cer* TALEN F1 animal screening (a) and genotype determination (b). Genotypes of twenty-nine animals were first analyzed using PCR product cleavage assay, and the animals carrying mutations at the target locus (marked by arrows) were further determined by DNA sequencing. Among the seven animals carrying mutations, three are $Cer^{-7/0}$ heterozygotes (showing a deletion of 7 bp in panel b) and one is a $Cer^{-12/0}$ heterozygote. The three $Cer^{-7/0}$ heterozygotes were used for further analysis in this study.

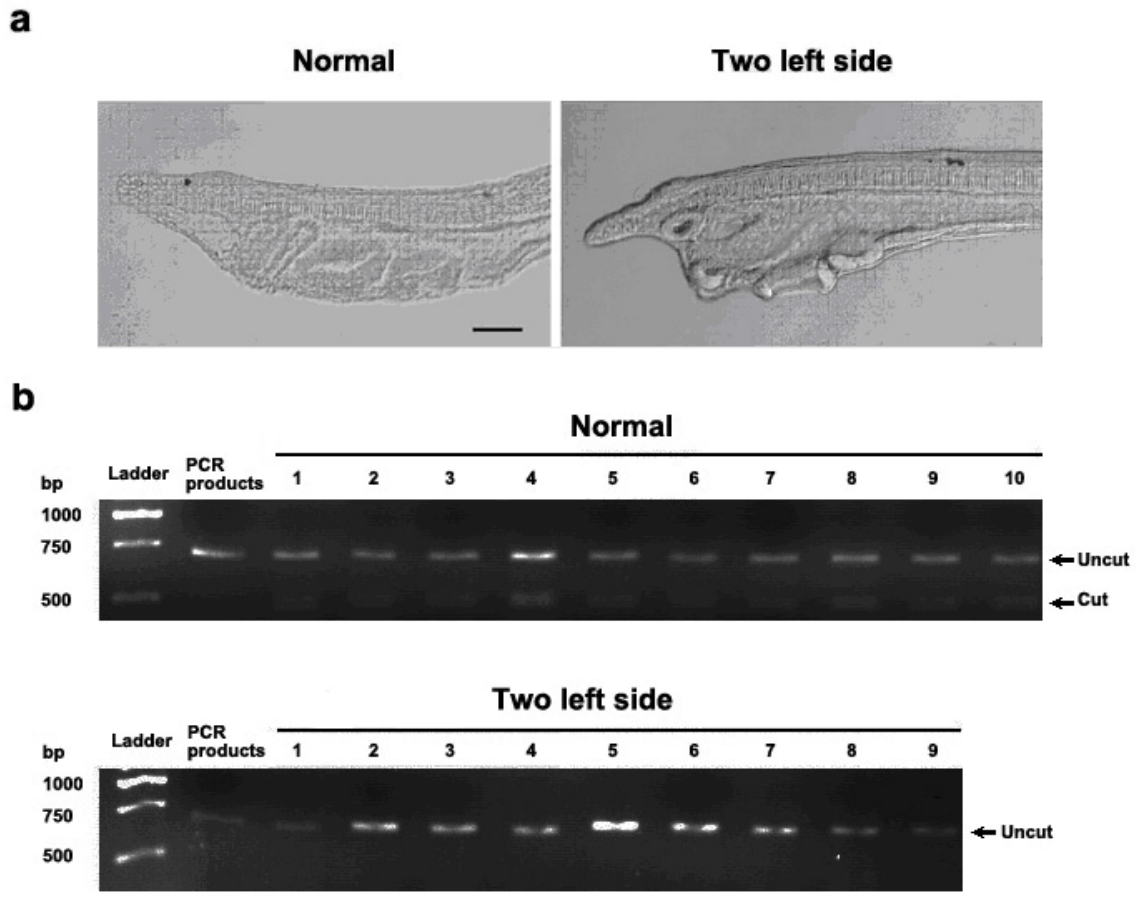

Fig. S4. Phenotype (a) and genotype (b) of TALEN *Cer* F2 animals. (a) Phenotype analysis revealed that the offspring from *Cer*$^{-7/0}$ inbreeding were born according to the correct Mendelian ratio: among the 584 animals analyzed, 134 showed two left side phenotype (see also *SI Appendix*, Fig. S7 and Fig. S5), while all others showed a wild type phenotype with mouth formed on the left side and endostyle on the right. This dose not significantly differ from the expected Mendelian ration of 3:1 ($p>0.25$; Chi-squared test). (b) Genotype analysis of 19 larvae revealed that larvae with normal LR asymmetry are *Cer*$^{-7/0}$ heterozygous (10/10), while larvae with the two left side phenotype are *Cer*$^{-7/-7}$ homozygotes (9/9). PCR products amplified from each of these 19 larvae were first digested with *Eag*I enzyme and then analyzed by gel electrophoresis. As shown in the image, about half of the PCR products deriving from larvae with normal phenotype (lanes 1-10) were digested by *Eag*I, but all of the product from larvae with the two left side phenotype were uncut.

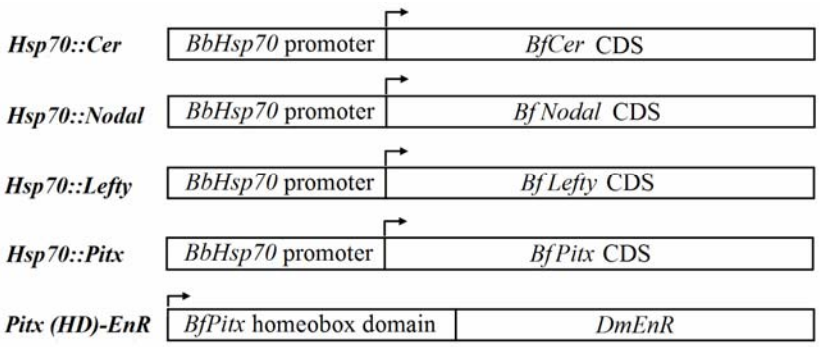

Fig. S5. Schematic representation of *Hsp70::Cer/Nodal/Lefty/Pitx* and *Pitx (HD)-EnR* constructs. Arrows indicate the transcription start sites. For *Hsp70::Cer/Nodal/Lefty/Pitx* constructs, transcription is driven by *B. belcheri Hsp70* gene promoter, and for *Pitx (HD)-EnR* construct, transcription is driven by a T7 promoter for in vitro RNA synthesis.

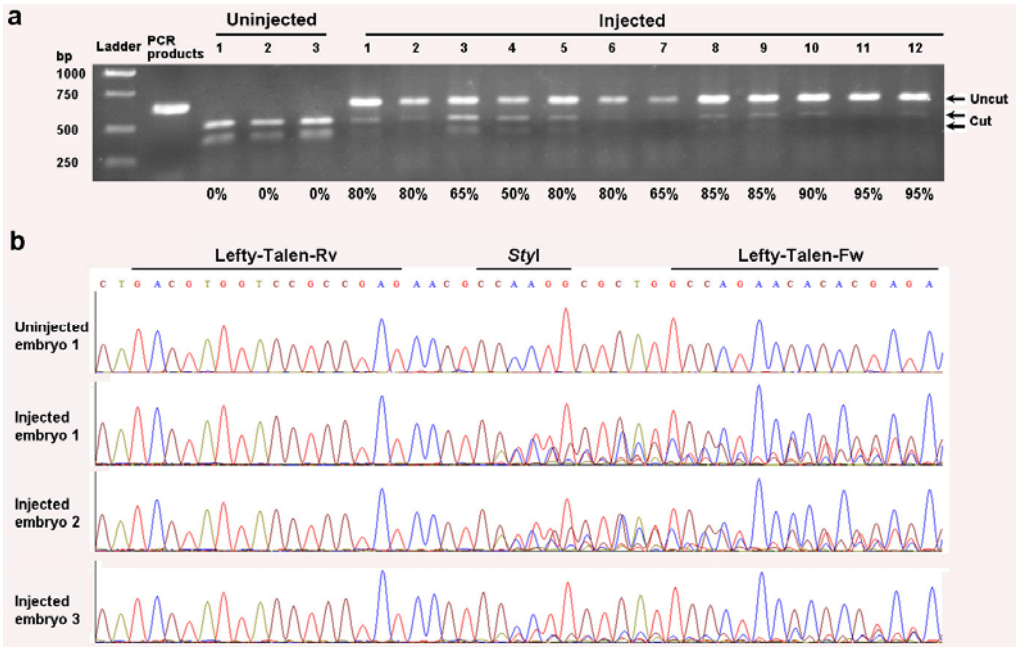

Fig. S6. Mutation ratios (a) and target sequences (b) of *Lefty* TALEN mRNA injected embryos. The mutation ratios of each embryo are assessed with PCR-restricted digestion since injection of TALEN mRNA into a zygote usually generates a mosaic individual. After injection with *Lefty* TALEN mRNAs, three un-injected and twelve injected embryos with normal morphology were randomly selected at mid-neurula stage and lysed separately using Animal Tissue Direct PCR Kit (Foregene Co., China). Fragments spanning the target site were amplified and then digested with restriction enzyme *Sty*I. The mutation efficiencies of each embryo were estimated by uncut:cut ratios shown under the gel image. As shown in image (a), PCR products from the three un-injected embryos were completely digested and more than 50% of PCR products from injected embryos were uncut. To verify the targeting specificity, the PCR products from the uninjected embryo 1 and three injected embryos were directly sequenced. As shown in image (b), the uninjected embryo 1 displays a uniform single peak throughout the sequence, and three injected embryos show multiple peaks after mutation site, indicating a site specific mutation.

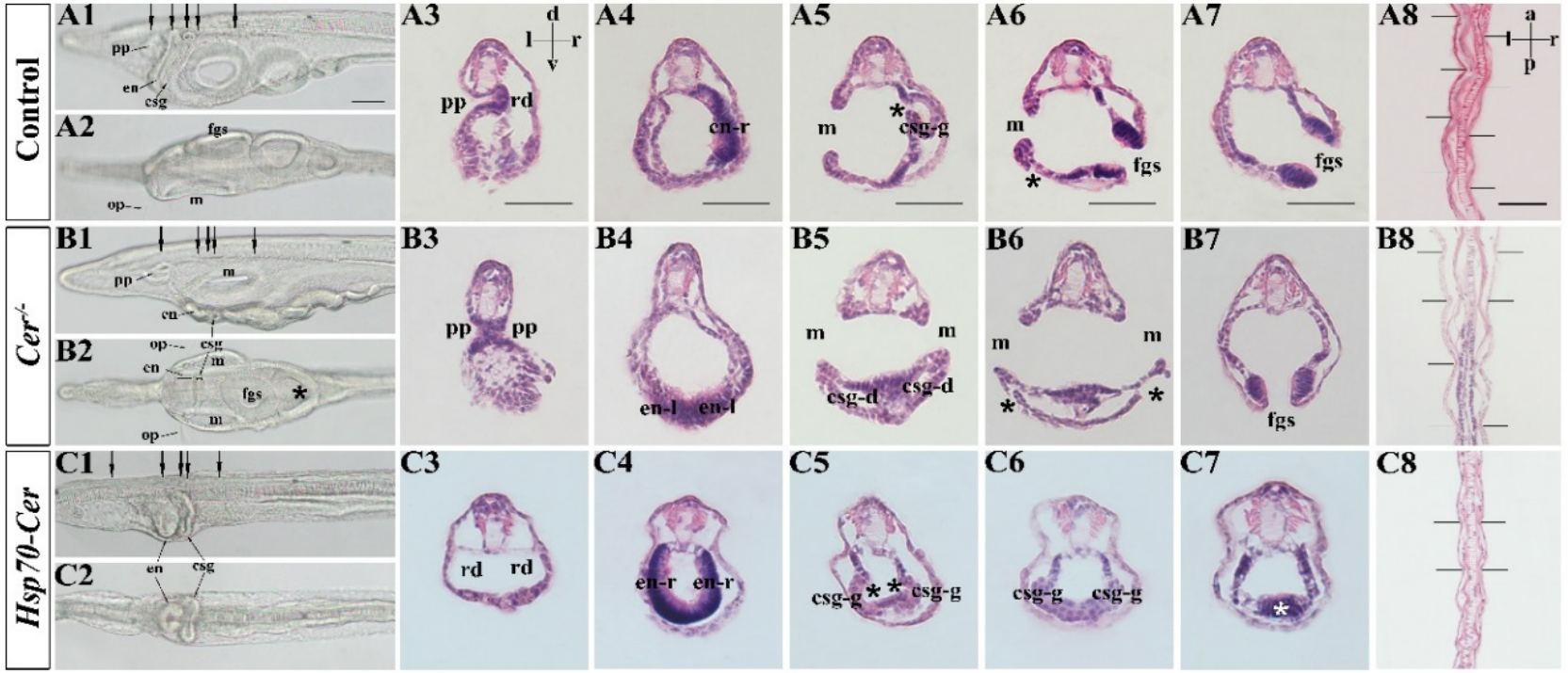

Fig. S7. *Cer* mutation or misexpression causes LR defects in amphioxus larvae. Panels A1, A2, A6, B1, B2, B6, C1, C2 and C6 are replicated from Fig. 4 for comparison. (A1-A8) Asymmetrical morphologies of control larvae (as seen in wild-type, *Cer*$^{+/-}$ or *Hsp70*::*Cer*-injected but not heat-hocked larvae). (A1) Left lateral view of pharyngeal region focused on the right side, showing the left-sided pre-oral pit (pp), right-sided endostyle (en) and club-shaped gland (csg). Arrows mark the section planes in (A3-A7). (A2) Dorsal view of pharyngeal region focused on the ventral side, showing the left-sided mouth(m) and oral papillar (op) and right-sided first gill slit (fgs). (A3) shows the left-sided pre-oral pit (pp) and right-sided right diverticulum (rd); (A4) shows the right part of endostyle (en-r); (A5) shows the left-sided mouth (m) right-sided glandular region of CSG (csg-g) and its internal opening (asterisk); (A6) shows the left-sided mouth (m), the external opening of CSG (asterisk) and the right-sided the first gill slit (fgs). (A7) shows the right-sided first gill slit (fgs). (A8) Longitudinal section of a 3-gill-slit-stage larva, showing the asymmetrical arrangement of the somites along A-P axis. (B1) Left lateral view of pharyngeal region focused on the sagittal plane, showing the left-side pre-oral pit (pp), mouth (m) and improperly developed endostyle (en) and CSG. Arrows mark the section planes in (B3-B7). (B2) Dorsal view of pharyngeal region focused on the ventral side, showing the duplicated mouths (m), oral papillae (op), left-side parts of the endostyle (en), CSG, and ventrally located the first (fgs) and second (asterisk) gill slits. (B3) shows the duplicated pre-oral pits (pp); (B4) shows the morphological symmetry of endostyle, resulting from the duplication of left-side endostyle (en-l); (B5) and (B6) show the duplicated mouths and ducts of

the CSG (csg-d). Two external openings of CSG (asterisks in B6) appear on both sides; (B7) shows the first gill slit (fgs) ventrally located. (B8) Longitudinal section of 3-gill-slit-stage *Cer* mutant larva, showing the symmetrical arrangement of somite along theA-P axis. (C1) Left lateral view of pharyngeal region focused on the sagittal plane, showing the improperly developed endostyle (en) and CSG (csg). No mouth opening and pre-oral pit are observed. Arrows mark the section planes in (C3-C7). (C2) Dorsal view of pharyngeal region focused on the ventral side, showing the morphological symmetry of endostyle and CSG, resulting from duplication of the right-side parts of endostyle and CSG. (C3) shows the duplicated right diverticulum (rd); (C4) shows the morphological symmetry of endostyle, resulting from the duplication of right-side part endostyle (en-r); (C5) and (C6) show the symmetrical feature of CSG, resulting from the duplication of right-sided glandular region (csg-g). Two internal openings of the CSG (asterisks in C5) appear on both sides; (C7) shows the first gill slit ventrally located. (C8) Longitudinal section of 3-gill-slit-stage *Cer* misexpressed larva, showing the symmetrical arrangement of somite along theA-P axis. All scale bars are 50 μm and are applicable to the panels in same column. Direction indicated in panel A3 (d, dorsal; v, ventral; l, left; and r, right) applies to all panels in the five middle columns, and that in panel A8 (a, anterior, p, posterior, l, left; and r, right) applies to panels B8 and C8. Black horizontal lines in A8, B8 and C8 mark the boundary between somitic segments